Comparative analysis of supercritical CO2 cycles

Jaroslaw Milewski[1*][✉], Arkadiusz Szczesniak [1], Kamil Futyma [1], Piotr Lis[1], Olaf Dybiński [1], Lukasz Szablowski [1], Marcin Wolowicz [1]

[1]Warsaw University of Technology, Faculty of Power and Aeronautical Engineering, Institute of Heat Engineering, 00-665 Warsaw, 21/25 Nowowiejska Street, Poland

✉ Jarosław.milewski@pw.edu.pl

Abstract

The presents a simulation of three different configurations of super critical CO_2 cycles: pre–compression, partial cooling, and recompression performed using commercially available software (Ebsilon). The highest thermal efficiency is obtained for the recompression cycle (35%). All three cycles operate at 700℃. In addition to enjoying the highest efficiency, the recompression cycle involves a moderate number of elements - just one heat exchanger more than the simplest cycle (Pre-compression).

Introduction

With rising energy demands and limited fossil fuels ([1]; [2]; [3]), there is a drive to find alternative energy sources such as hydrogen fueled gas turbines ([4]; [5]), solar power ([6]; [7]), wind power ([8]), fuel cells ([9]; [10]; [11]; [12]; [13]; [14]; [15]; [16]; [17]; [18]; [19]; [20]; [21]; [22]; [23]; [24]; [25]; [26]; [27]; [28]; [29]; [30]; [31]; [32]; [33]; [34]; [35]; [36]), etc. The problem can be partially solved by introducing new energy carriers as alternative fuels ([37]; [38]; [39]), which can be converted into hydrogen ([40]) as an alternative to electrolysis ([41]; [42]) or be used to store energy in other forms ([43]; [44]; [45]). Thus, in addition to introducing low energy consumption technologies, it is also very important to boost the efficiency of power sources. Waste heat recovery with thermal energy storage ([46]) is one way to address two contrasting goals: mitigating greenhouse gas emissions out of climate change concerns while supplying energy to favor economic growth ([47]) and so meet increasing demands for industrialization and social development ([48]). But this does not solve the problem of rising electricity demands. Conversion of waste heat into electricity, however, looks promising. When we look at a classical power system such as gas-fired turbines, the pure balance of power shows that the component with the highest power demand in such a system is the air compressor, which consumes up to 75% of turbine power. Lowering this demand can be done by keeping the compressor close to the critical point of the working fluid, thus power consumption will be comparable to a pump in Rankine cycles. To do so and still be at the ambient temperature level, the working fluid should be carefully selected. One of the candidates is carbon dioxide.

In the 1960s, Feher ([49]) studied the properties of various gases with a view to determining the most suitable one for a supercritical thermodynamic cycle. Carbon dioxide was proposed as a working fluid for several reasons. First, its physical properties e.g. critical pressure, which is significantly lower than water, allow the system to work at lower operating pressures. Second, the thermodynamic and transport properties of CO_2 are well known, hence cycle analysis is based on reasonably firm data. Finally, carbon dioxide is abundant, non-toxic and relatively low cost. The analysis proved that the CO_2 supercritical cycle offers several desirable features: high thermal efficiency (the investigated cycle achieved thermal efficiency of 55% under ideal conditions), low volume-to-power ratio and no blade corrosion or cavitation. The paper suggests using it for electric power

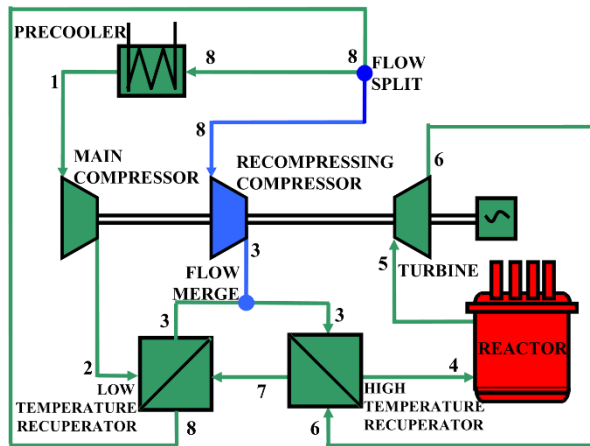generation (both terrestrial and space) and to provide shaft power for marine propulsion.

Figure 1: Recompression Brayton cycle layout ([50])

Research on supercritical CO_2 power cycles was resumed by Dostal four decades later. In 2004 ([50]) he performed a systematic, detailed major component and system design evaluation and multi-parameter optimization of the family of supercritical CO_2 Brayton power cycles for application to advanced nuclear reactors. His analysis showed that the recompression cycle shown in Figure 1 was the best performing cycle layout due to its simplicity, compactness, cost and thermal efficiency. Three direct cycle designs of this layout were selected for further investigation. They achieved thermal efficiencies of 45.3, 50 and 53%, assuming turbine inlet temperatures of 550, 650 and 700°C respectively. According to the analysis the turbomachinery is highly compact—the 600 MWth/246 MWe power plant is fitted with a turbine of 1.2 m in diameter and 0.55 m long, which translates into power density of 395 MWe/m^3.

Later, Driscroll ([51]) presented a report on cost projections for the supercritical CO_2 Brayton indirect power cycle as applied to GEN-IV advanced reactors. In order to evaluate the economic competitiveness of the cycle a cost comparison procedure was adopted in which projections were made on the basis of published cost estimates for related reactor systems coupled with the direct or indirect helium Brayton cycle or the conventional indirect Rankine cycle. A preliminary

analysis showed savings of at least 10%, with the dominant parameters being cycle thermodynamic efficiency and turbomachinery capital cost.

These two papers have spawned a number of further studies of the CO_2 supercritical cycle in the field of parameters and layout optimization, possible applications and modeling of critical cycle components.
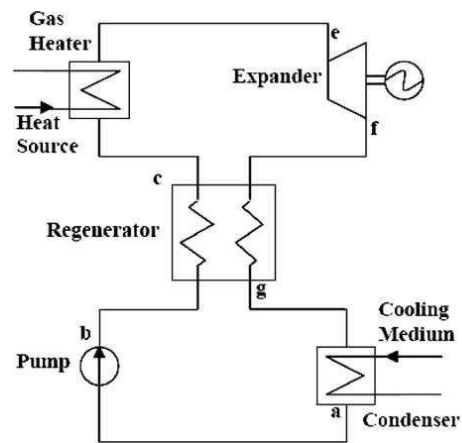

Figure 2: CO_2 transcritical system layout and cycle T-S chart ([52])

Chen ([52]) evaluated transcritical CO_2 as a working fluid in low-grade waste heat recovery cycles by comparing it to R123 Organic Rankine Cycle (ORC). Figure 2 shows the basic ORC system layout and the ORC schematic cycle in a T–S chart. The results of the comparison showed that, when utilizing a low-grade

heat source with equal thermodynamic mean rejection temperature, the CO_2 transcritical cycle has slightly higher power output than ORC and is more compact as well. On the other hand, further research carried out by Vidhi et al. in 2011 ([53]) showed that although CO_2 enjoys the advantages of being economically favorable, environmentally safe and available in abundance, its performance in a transcritical power cycle is not as efficient as an R32 based organic Rankine cycle over the range of heat source temperatures from 140°C to 200°C A comparative analysis of a recompression CO_2 Brayton cycle combined with ORC and a single recompression cycle was also performed.

It showed that the exergy efficiency of the combined cycle could be higher than that of the single recompression cycle by up to 11.7% and the total product unit cost lower by up to 5.7% ([54]).

Parametric optimization performed by Wang et al. ([55]) using a genetic algorithm and artificial neural network showed that the key thermodynamic parameters, such as turbine inlet pressure, turbine inlet temperature and environment temperature have a significant effect on the performance of a supercritical CO_2 power cycle and exergy destruction in each component.
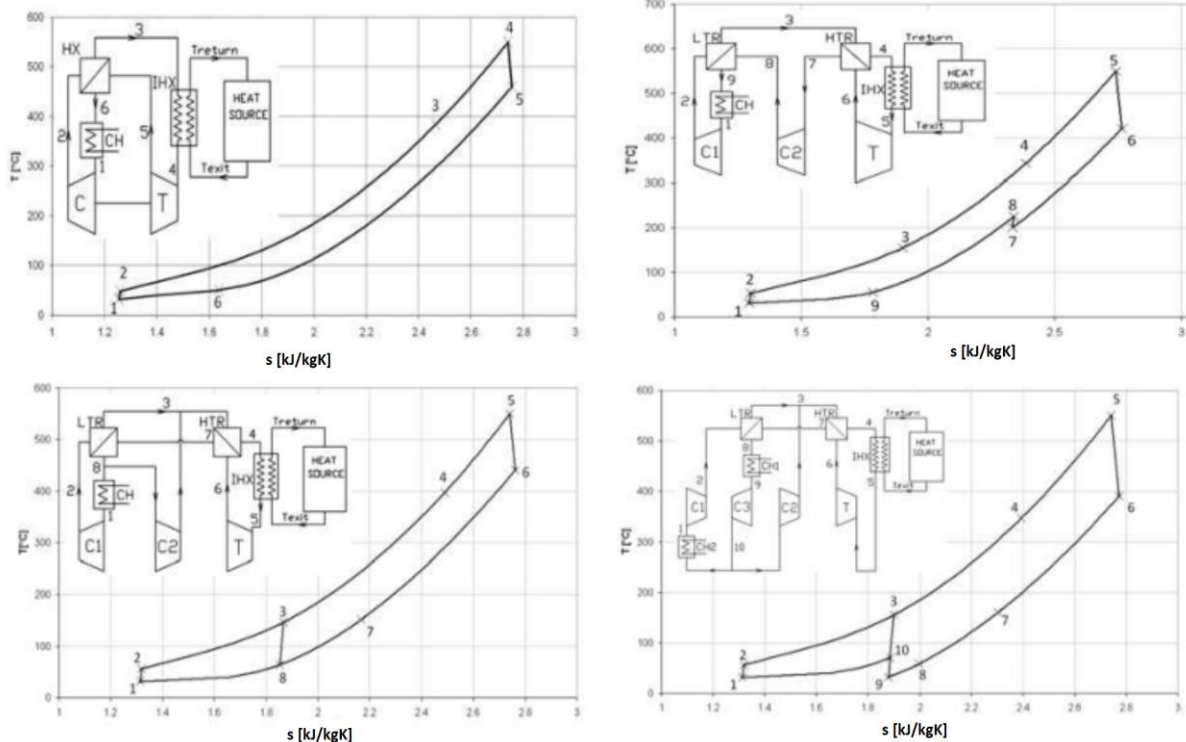

Figure 3: Simple Brayton, Precompression, Recompression and Partial Cooling cycle

Kulhanek and Dostal found that of the various cycle layouts shown in **Error! Reference source not found.** the recompression Brayton cycle achieves the highest efficiency in the range of turbine inlet temperatures between 500 and 600°C, whereas the partial cooling cycle is better at higher temperatures. On the other hand, Bryant ([56]) proved that, indeed, the recompression cycle will always be more efficient than a simple cycle provided that the two cycles have the same precooler inlet temperature, but in order to

satisfy this condition the recompression cycle will always require more total recuperator area. The paper demonstrated that when two cycles are compared on the basis of equal total recuperator area, the efficiency advantage of the recompression cycle is substantially reduced or even disappears altogether.

Kim and Favrat in 2012 ([57]) presented a novel transcritical Rankine cycle using both low and high temperature heat sources to maximize the power output of the CO_2 power cycle with a given high temperature source for use in applications such as

nuclear power, concentrating solar power and combustion. The analysis showed the large internal irreversibility in the recuperator related to the higher specific heat of the high-pressure side than that of the low pressure side. Additional low temperature heat provided to the recuperator in the proposed cycle mitigates the specific heat difference, and thus makes it possible to achieve higher recuperator CO_2 outlet temperatures. This feature in conjunction with reduced compression work and exergy losses makes the low-high temperature Rankine cycle even more effective than the recompression Brayton cycle.

Application of supercritical CO_2 cycles in a cogeneration power plant was considered by Moroz in 2014 ([58]). The performance of several stand-alone supercritical CO_2 cycles and combined steam/supercritical CO_2 cycles was compared with typical steam cogeneration cycles. The cascaded supercritical CO_2 recompression Brayton cycle achieved the best electrical efficiency of 39.4% at turbine inlet temperature of 540°C, which beat the ordinary steam CHP unit.

Figure 4: Simple Brayton, Precompression, Recompression and Partial Cooling cycle [60]

In 2009 Moisseytsev ([59]) examined alternative supercritical CO2 Brayton cycle layouts, which were presumed to perform better than the recompression Brayton cycle when coupled with Sodium Fast Reactors. This assumption was since SFRs operate at lower temperatures (core outlet temperature of 510°C) than the temperature for which a satisfactory recompression cycle performance had been proved. Even though a double recompression cycle intercooling between compressor stages and reheating between high and low pressure turbine was analyzed, the recompression cycle demonstrated the highest efficiency. Later, Perez-Pichel ([60]) conducted a similar analysis in which he compared a wide range of configurations, from the simplest one to combined cycles (with organic Rankine cycles, ORC). As a result, he discovered that the most basic layouts (such as the recompression cycle and basic combined ORC cycle) could reach thermal efficiency as high as 43.3%, which is comparable to efficiencies obtained through supercritical steam Rankine cycles. The simplest combined cycle, which achieved the highest efficiency, is presented in Figure 4.
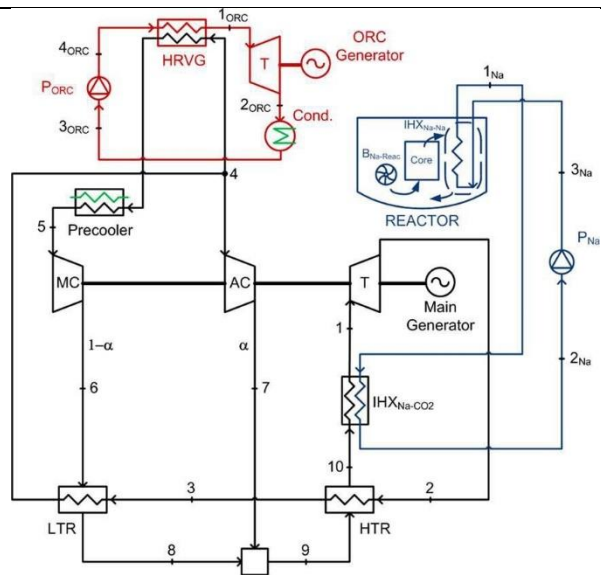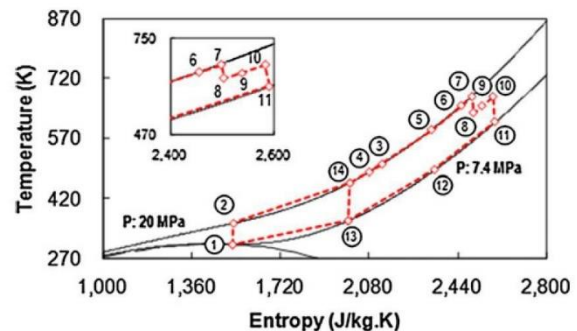

Figure 5: T–s diagram of the recompression cycle with reheating ([62])

Harvego and McKellar ([61]) performed a comparative study of the direct and indirect recompression Brayton cycle coupled to a nuclear reactor. Both layouts were examined in the same conditions, i.e., operating Brayton cycle pressure of 20 MPa and reactor outlet temperature between 550 and 850°C. The results of the analysis showed that, for the direct supercritical CO_2 power plant cycle, thermal efficiencies in the range

of 40 to 50% could be achieved over the assumed reactor coolant outlet temperature. For the indirect supercritical power plant cycle, thermal efficiencies were approximately 11..13% lower than those obtained for the direct cycle over the same core outlet temperature range. In 2012 Halimi ([62]) conducted a computational analysis of the supercritical CO_2 Brayton cycle power conversion system for fusion reactor application. The analysis results showed that thermal efficiency of 42.44% was achievable for a recompression cycle. Additional 0.69% benefits can be obtained by adopting the reheating concept shown in Figure 5. Yoon et al. ([63]) suggested coupling a supercritical CO2 cycle with small and medium sized water-cooled nuclear reactors (SMR). According to the cycle evaluation, the maximum cycle efficiency at a temperature of 310°C and compressor outlet pressure of 22 MPa is 30.05%, which is comparable to the efficiency of current steam Rankine cycles. Moreover, the total volume of turbomachinery which can service 330 MWth of SMR is less than 1.4 m^3 excluding the casing.

Besides the studies of the supercritical CO_2 cycle as a nuclear application, a number of analyses of these novel cycles coupled with Concentration Solar Power have been performed. Zhang and Yamaguchi conducted three successive semi-experimental studies using a real Rankine cycle with a relief valve as a counterpart of a turbine. They accomplished maximum CO_2 temperature of 165°C at the collector outlet ([64]), which achieved theoretical electric output efficiencies of 11.4% ([65]) and 11.6% ([66]) in the next study. These efficiencies were slightly higher than those obtained by the solar cell used in the experiment for the purpose of comparison.

Figure 6 shows a new type of solar energy-based power generation using supercritical CO_2 and heat storage. The calculations performed showed that the supercritical CO_2 Rankine cycle not only achieves higher energy conversion efficiency than conventional water-based systems, but also overcomes the intermittent nature of solar energy. The paper also proved that the efficiency of the expander and the performance of the heat storage/regenerator have significant effects on the system's overall performance, while the pump is relatively unimportant ([67]).
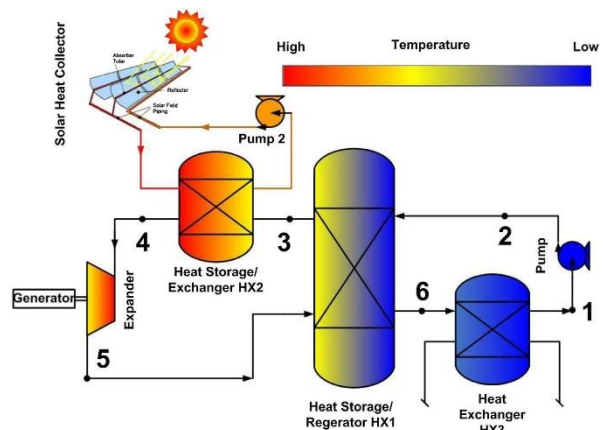

Figure 6: Schematic diagram of a solar energy storage and power generation system based on CO_2 ([64])

Iverson and Cowboy in ([68]) supported the statement above, emphasizing good cycle efficiency especially over 600°C. They used an experimental loop installed in Sandia National Laboratories, which was the split flow supercritical CO_2 Brayton cycle shown in
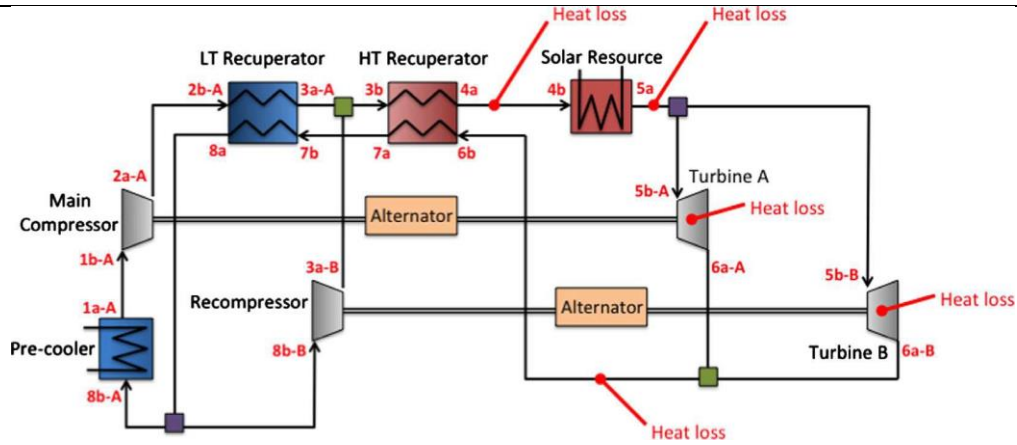
Figure 7: Layout of split-flow recompression Brayton cycle components ([68])

. The experiment showed good cycle behavior as a response to intermittent heat supply. Measurements of the system indicated an overall efficiency of approximately 5% for the operating conditions used in the experiment. However, the authors expected this efficiency to increase to 15% at design conditions and to approximately 24% with minor modification to improve insulation.

In 2015 Padilla et al. ([69]) analyzed the effect of turbine inlet temperatures and the cycle configuration on the thermal performance and exergy destruction of a supercritical CO_2 cycle within a CSP central receiver application. They found that the thermal efficiency of the supercritical Brayton cycle increases monotonically with the temperature of the cycle. The recompression cycle with main compressor intercooling achieved the best thermal performance (55.2% at 850ºC). However, Cheang et al. ([70]) in their study of the same year argued that although the supercritical CO_2 cycle looks attractive, it is still both less efficient and less cost competitive than a superheated steam Rankine cycle.
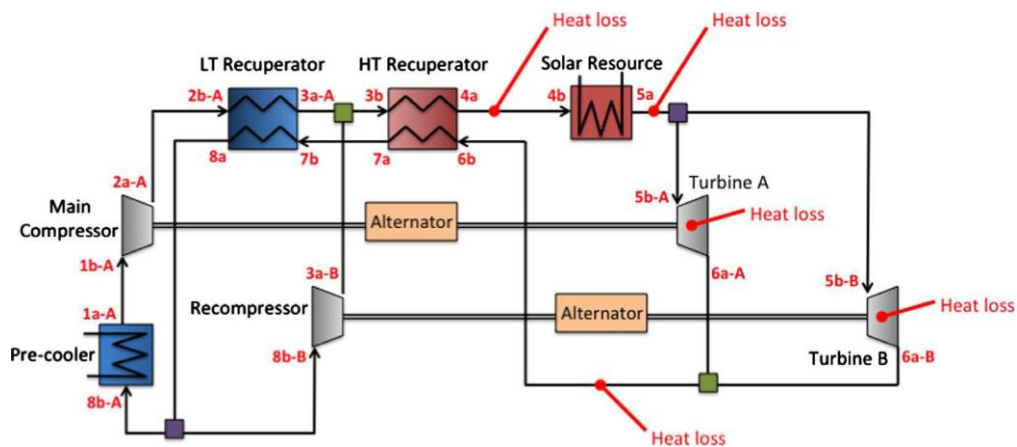

Figure 7: Layout of split-flow recompression Brayton cycle components ([68])

The next area in which research has been carried out is a supercritical CO_2 cycle application as a bottoming cycle within fuel cells ([71]) systems. Sanchez et al. in 2009 ([72]) expected a CO_2 cycle to perform better for intermediate temperature heat recovery applications than an air cycle. Their paper showed that, even though the new cycle is coupled with an atmospheric fuel cell, it is still able to achieve the same overall system efficiency and rated power than the best conventional cycles currently being considered. Furthermore, under certain operating conditions, the performance of the new hybrid systems beats that of existing pressurized fuel cell hybrid systems with conventional gas turbines. Calculations carried out by Muńoz de Escalona ([73]) proved that an indirect supercritical CO_2 Brayton cycle coupled to a Molten Carbonate Fuel Cell (MCFC) can achieve thermal efficiency of almost 40%, which enables the whole system to approach overall efficiency of 60%. In addition, the supercritical CO_2 cycle performs better at part load than existing hybrid systems.

Bae et al. compared various cycle layouts presented in Figure 8 in terms of application as an MCFC bottoming cycle. The results showed that all of the analyzed sCO2 Brayton cycle layouts perform better than the air Brayton cycle ([75]), in particular the recompression Brayton, the cascading Brayton and the Rankine cycles can increase net hybrid system efficiency by over 10% more than the single MCFC system. ([74])

Another avenue of research concerns the use of a supercritical CO_2 cycle in coal applications. Moullec ([76]) adapted a supercritical CO_2 Brayton cycle to the coal-fired boiler thermal output shown in Figure 9. An energy evaluation of the overall power plant indicated net power plant efficiency of 41.3% with carbon capture ([77]), and CO2 compression to 110 bar. Moreover, a technical-economic analysis of a designed power plant showed a levelized cost of electricity (LCOE) reduction of 15% compared to a reference supercritical coal-fired power plant equipped with a standard carbon capture process. A further study showed that the oxy-combustion cycle seems the best fitted for the supercritical CO_2 Brayton cycle due to the simpler thermal integration and the CO_2 purification devices already integrated in the CO_2 processing unit. However, the main technological challenges were also identified, namely, the very large exchanger needed in the cycle to achieve high power cycle efficiency, and the development of a supercritical CO_2 turbine, which differs significantly from steam or gas turbines especially due to the very large effort on the wheel and the small size of the equipment ([78]).
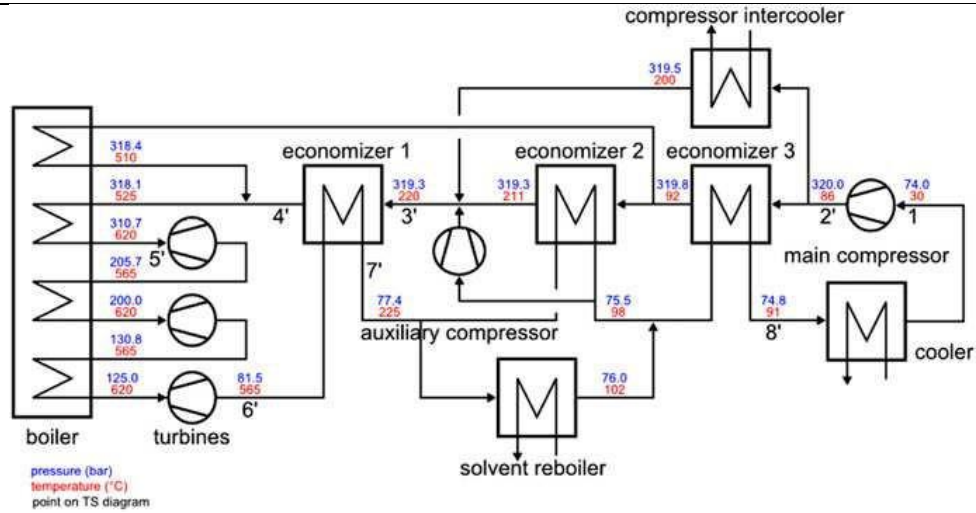
Figure 8: Supercritical Brayton CO$_2$ power cycle adapted for a coal-fired boiler with carbon capture ([76])
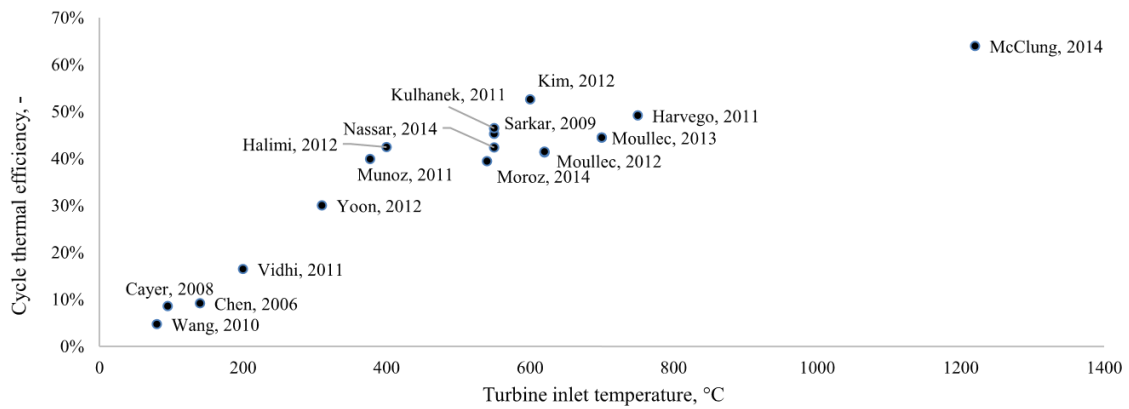

Figure 9 General correlation between cycle efficiency and turbine inlet temperature in multiple studies ([54]; [74]; [56]; [70]; [79]; [80]; [73]; [81]; [82]; [62]; [61]; [68]; [57]; [67]; [32]; [59]; [58]; [78]; [76]; [69]; [60]; [72]; [83]; [55]; [64]; [63]; [65] ; [66])

Although some supercritical CO_2 cycles, such as the recompression cycle, exhibit high efficiency, they utilize a high degree of recuperation leading to a narrow change across the thermal input device. This narrow window may be acceptable for waste heat and nuclear applications, but it is not suitable for a traditional coal or natural gas fired system. McClung ([32]) proposed two cycles: Cryogenic Pressurized Oxy-Combustion (CPOC) and Advanced Supercritical Oxy-Combustion (ASOC). The calculations performed showed that, for both direct cycles, turbine inlet temperature of 1,220°C enables power block thermal efficiencies of near to 64% and overall power plant efficiency exceeding 52%. However, the CPOC cycle seems to be more attractive due to the wider thermal input window, which leads to simpler combustor designs and more efficient usage of fossil based thermal input.

The results of the most significant studies referenced above, are plotted in the coordinate system presented in Figure 11, where the x and y axes correspond to turbine inlet temperature and cycle efficiency, respectively. A positive correlation between these two parameters can be seen in the chart.

Comparative analysis of supercritical CO_2 cycles

The most basic and compact supercritical CO_2 cycle is a simple Brayton cycle. It is simple and offers relatively good efficiency. However, there is still potential to improve its performance. The biggest reduction in efficiency of the supercritical Brayton cycle comes from the large irreversibility in the recuperator ([81]). Compound cycles have been introduced to overcome this problem and as shown later on in this paper, these cycles perform significantly better than the regular supercritical Brayton cycle.

Pre-compression cycle

The pre-compression Brayton cycle is one of the ways to increase generation within the cycle and reduce the pinch point problem. As shown in Figure 11 the cycle is similar to the normal Brayton cycle with a small modification. First, the working fluid is compressed

and then heated in the high temperature recuperator (1) using exhaust heat from the turbine. The fluid passes to a heat source (2), where heat is added, and then expands in the turbine (3). The remaining exhaust heat is extracted from the fluid in the high temperature recuperator (1). The difference from the normal Brayton cycle is that in the middle of the recuperation process, when the hot fluid temperature approaches the heated fluid temperature, a compressor (5) is introduced that compresses the fluid to a higher pressure. As the fluid pressure rises, so does its temperature and specific heat. Thus, the regeneration process can continue, and more available heat is returned to the heated fluid. This extra heat reduces the average temperature at which heat is rejected from the cycle and increases the average temperature at which heat is added to the cycle. This results in an efficiency improvement of 6% over a Brayton cycle that would otherwise suffer from the pinch point problem ([84]).
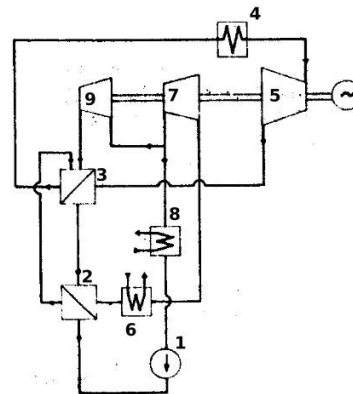
Partial cooling cycle

Figure 10 Layout of split-flow recompression Brayton cycle components ([81])

Another cycle layout that aims at reducing Brayton cycle drawbacks is the partial cooling cycle presented in Figure 10. In general, its operation differs from the previously described cycle in terms of two adjustments. The first is that only a fraction of the working fluid is compressed in the low temperature compressor (pump). The rest is compressed in the recompression compressor that is introduced before the pre-cooler and after the pre-compression compressor. The second difference is the introduction

of another pre-cooler before the pre-compression compressor. This way, similar to the pre-compression cycle, more heat is available for the regeneration process.

After compression in the main compressor (1), a fraction of the working fluid is heated in the low temperature recuperator (2) and merged with the flow from the re-compressing compressors, which is at the same conditions. The fluid is then heated in the high temperature recuperator (3) and in the heat source (4) in turn and then enters the turbine (5). After the expansion process the fluid returns its heat in the high and low temperature recuperator (2,3). Then it passes to the pre-cooler (6) where it is cooled to the pre-compressor inlet temperature, and subsequently compressed in the pre-compressor (7). A part of the pre-compressed fluid is sent to the pre-cooler (8) and the main compressor. The rest is recompressed in the second recompressing compressor (9) to the high temperature recuperator inlet conditions, and then is merged with the stream from the main compressor. This move eliminates the pinch point problem, since due to the lower mass flow rate on the high-pressure side of the low temperature recuperator, the mass flow weighted heat capacity of the streams is about equal and a pinch point does not occur.

The cycle improves its efficiency by reducing the average temperature of heat rejection so that the efficiency improvement is bigger than that for the pre-compression cycle.

Recompression cycle

Although the partial cooling cycle looks attractive due to its efficiency benefits, the complication of the cycle layout may prove detrimental to the economic outcome. Therefore, another cycle is introduced, a recompression cycle, which is simpler than both the partial cooling and pre-compression cycle. The general layout of the cycle is shown in Figure 13.

The advantage of this cycle is that it eliminates one precooler and pre-compressing compressor from the cycle. After the regeneration process in the high temperature recuperator (3) the fluid is heated in the heat source (1) and passes to the turbine (2). Then it enters successively the high and low temperature recuperators (3,4) and returns its heat to the fluid on

the high-pressure side. The fluid flow is then split into two streams. The first is sent directly to the recompression compressor, where it is compressed to the same pressure conditions as the CO_2 leaving the main compressor and merged with it in the high pressure recuperator. The second flow is cooled in the precooler (5), compressed in the main compressor (6) and heated in the recuperators.
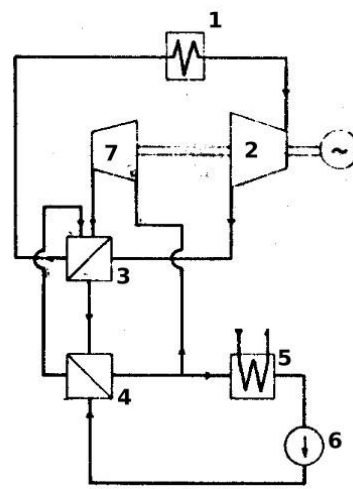

Figure 11 Schematic diagram of the recompression Brayton cycle ([81])

Table 1: Results comparison of various algorithms.

Parameter	Value
Turbine Inlet Temperature, °C	700
Turbine Inlet Pressure, MPa	20.2
Turbine Isentropic Efficiency, %	80
Compressor efficiency, %	85
Heat exchanger effectiveness	0.6

The effect of recompression is sufficient to overcome the pinch point problem. Owing to the decreased mass flow rate on the high-pressure side of the low temperature recuperator, the mass flow weighted heat capacity of the streams is about equal on both sides and a pinch point does not occur.

The recompression cycle is, along with the pre-compression cycle, the simplest among the surveyed cycles. In addition, at the desired operating conditions

of turbine inlet pressures and temperatures (20 MPa and 550°C), it achieves the highest efficiency of all examined cycles ([81]). Therefore, the recompression cycle is usually selected as the best-suited cycle and investigated with respect to various applications in the literature.

Modeling of supercritical CO$_2$ cycles

The main CO$_2$ cycles layouts presented here are simulated in EBSILON®Professional software to compare their performance based on the same mathematical model adopted in the simulation software. The CO$_2$ properties were simulated by means of "universal fluid" defined in the Refprop library, which is provided by EBSILON®Professional (version 12.01). The simulation of the most popular CO$_2$ layouts using the same simulation software and assumptions means a comprehensive comparison can be made of various CO$_2$ layouts, thereby eliminating the

inaccuracies which are inevitable when using different models created by various authors.

Table 1 summarizes the input variables and constants which were used for the comparison of layouts.

The schematic diagram of the cycles implemented in EBSILON®Professional are shown in the following Figures: pre-compression Brayton cycle—Figure 12, partial cooling Brayton cycle—Figure 14, recompression Brayton cycle—Figure 16. The operating parameters for each layout are shown in Figure 13 (pre-compression cycle layout), Figure 15 (partial cooling cycle layout), Figure 17 (recompression cycle layout).

The simulation results revealed that the most efficient cycle layout is the recompression Brayton cycle—see Table 2. The displayed values in Table 2 corresponds to cycles operating with the assumptions given in Table 1.
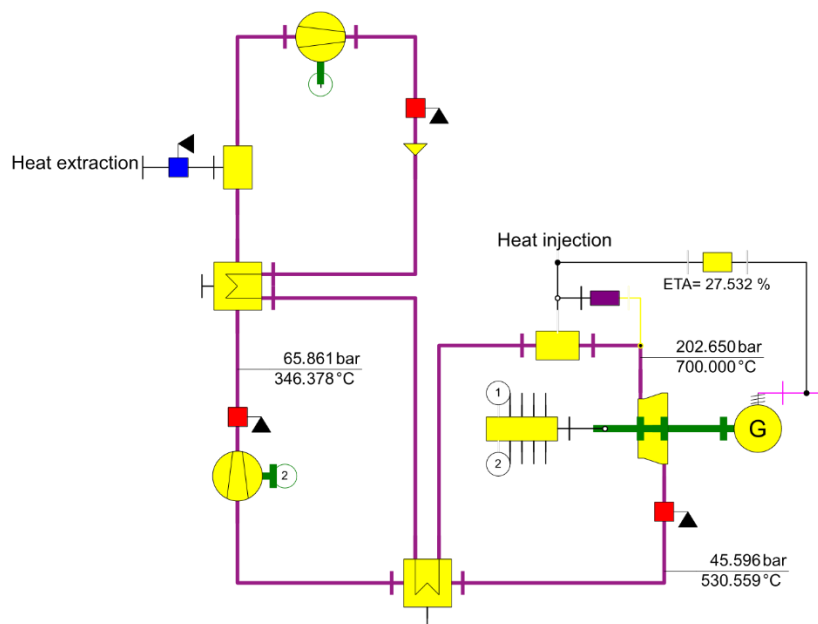

Figure 12 Schematic diagram of the pre-compression Brayton cycle implemented in Ebsilon software
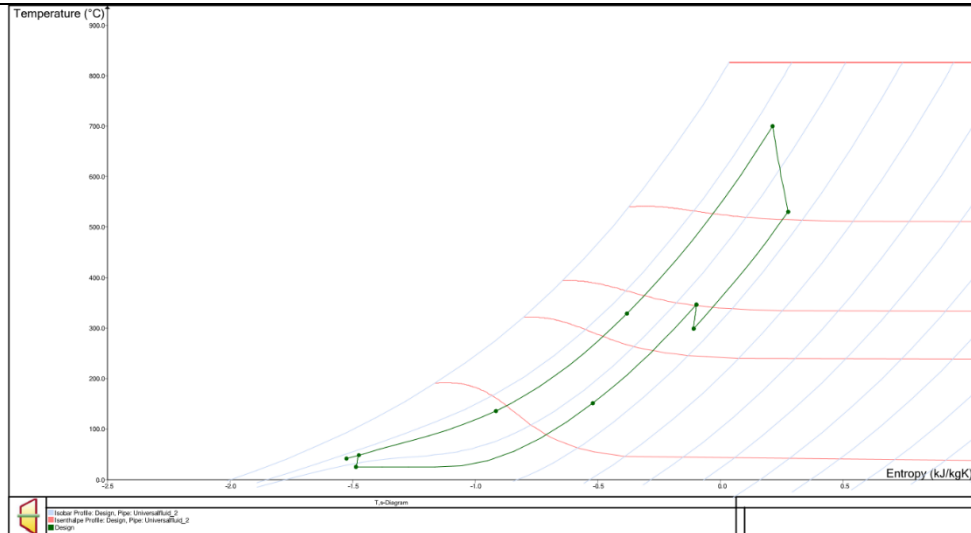
Figure 13 Temperature-entropy diagram of the pre-compression Brayton cycle implemented in Ebsilon software
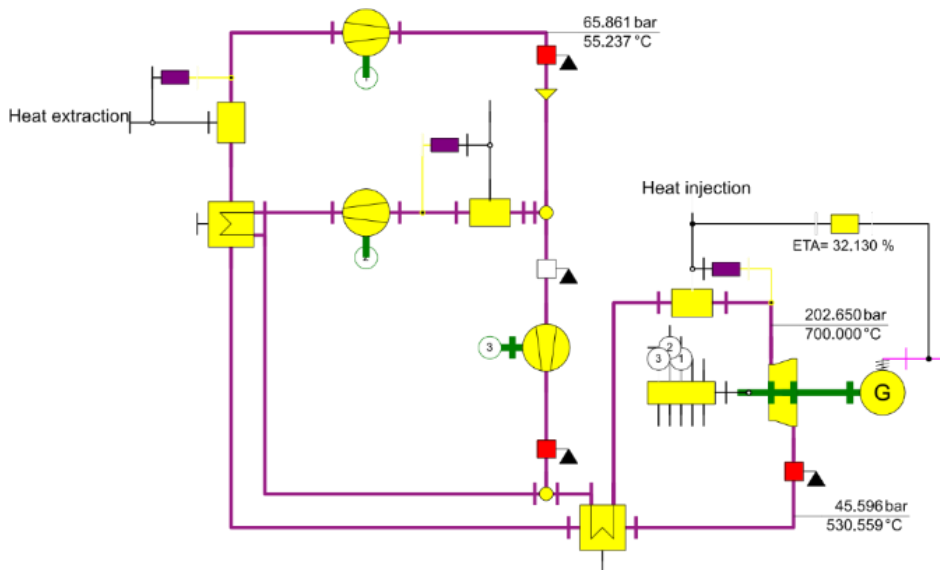

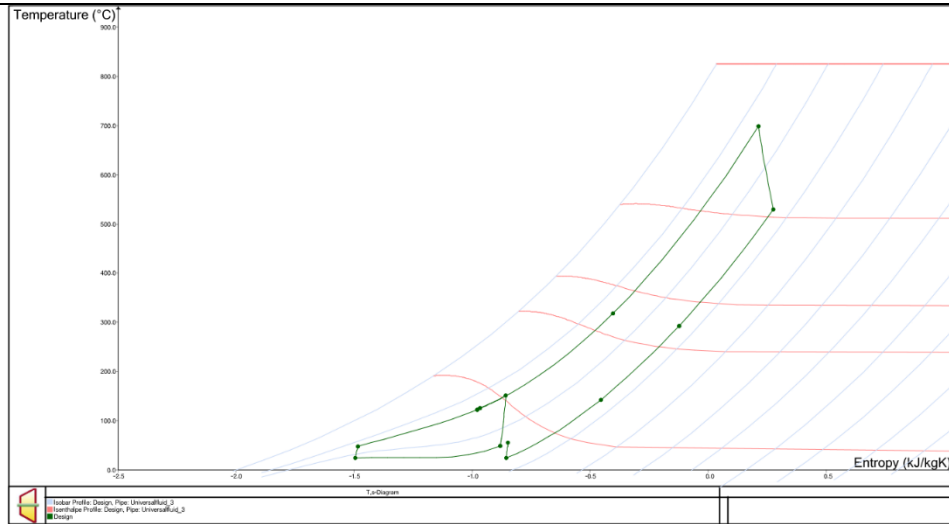*Figure 14 Schematic diagram of the partial cooling Brayton cycle implemented in Ebsilon software*

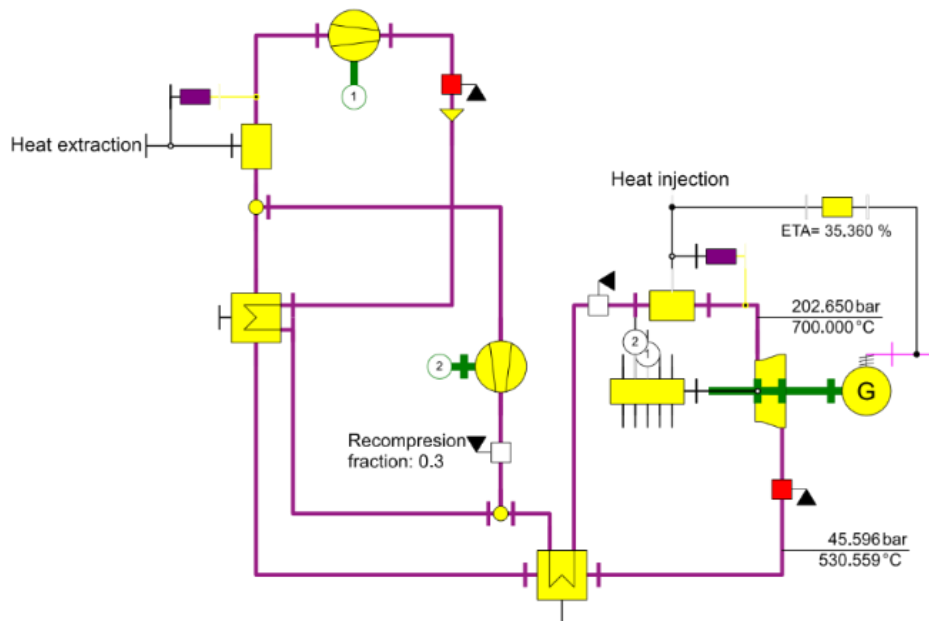*Figure 15 Temperature-entropy diagram of partial cooling Brayton cycle shown in T-s diagram*

Figure 16 Schematic diagram of the recompression Brayton cycle implemented in Ebsilon software
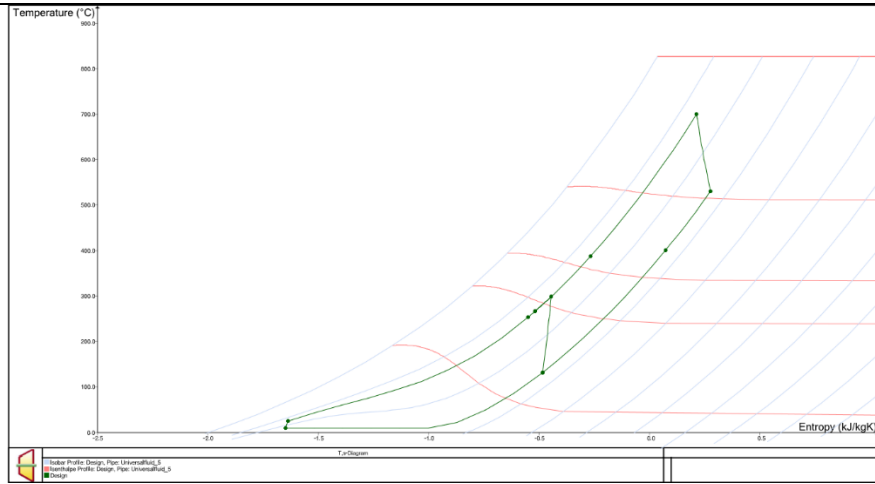
Figure 17 Temperature-entropy diagram of recompression Brayton cycle shown in T-s diagram

Table 2: Comparison of simulation results

Brayton cycle layout	Pre-compression	Partial cooling	Recompression
Cycle efficiency, %	27.5	32.1	35.4
Number of heat exchangers	2	1	2
Number of compressors	1	3	2
Number of expanders	1	1	1

The next step will be a detailed analysis of the Recompression Brayton cycle to identify its operational range in the off-design mode.

Conclusions

By using commercially available software (Ebsilon), we simulated three different configurations of super critical CO_2 cycles: pre-compression, partial cooling, and recompression. The highest thermal efficiency is obtained for the recompression cycle (35%). All three cycles operate at 700°C. We did not specify the form of the heat source, and it was assumed that this is the temperature of the working fluid (CO_2) at the expander inlet. The expander inlet pressure was kept at the same level for all three cycles.

In addition to enjoying the highest efficiency, the recompression cycle is composed of a moderate amount of elements – just one heat exchanger more than the simplest cycle (pre-compression).

Acknowledgments

References

[1]   Bartnik R, Buryn Z, Hnydiuk-Stefan A, Juszczak A. Methodology and a Continuous Time Mathematical Model for Selecting the Optimum Capacity of a Heat Accumulator Integrated with a {CHP} Plant. Energies 2018;11:1240. https://doi.org/10.3390/en11051240.

[2]   Plis M, Rusinowski H. A mathematical model of an existing gas-steam combined heat and power plant

for thermal diagnostic systems. Energy 2018;156:606–19. https://doi.org/10.1016/j.energy.2018.05.113.

[3]   Wu M, Zhang H, Liao T. Performance assessment of an integrated molten carbonate fuel cell-thermoelectric devices hybrid system for combined power and cooling purposes. Int J Hydrogen Energy 2017;42:30156–65. https://doi.org/10.1016/J.IJHYDENE.2017.10.114.

[4]   Kotowicz J, Bartela Ł, Dubiel-Jurgaś K. Analysis of energy storage system with distributed hydrogen production and gas turbine. Arch Thermodyn 2017;Vol. 38:65–87. https://doi.org/10.1515/AOTER-2017-0025.

[5]   Comparison of the Brayton–Brayton Cycle with the Brayton-Diesel Cycle | Journal of Power Technologies n.d.

[6]   Bonaventura D, Chacartegui R, Valverde JM, Becerra JA, Ortiz C, Lizana J. Dry carbonate process for CO2 capture and storage: Integration with solar thermal power. Renew Sustain Energy Rev 2018;82:1796–812. https://doi.org/10.1016/J.RSER.2017.06.061.

[7]   Siddiqui O, Dincer I. Analysis and performance assessment of a new solar-based multigeneration system integrated with ammonia fuel cell and solid oxide fuel cell-gas turbine combined cycle. J Power Sources 2017;370:138–54. https://doi.org/10.1016/J.JPOWSOUR.2017.10.008.

[8]   Clúa JGG, Mantz RJ, Battista H De. Optimal sizing of a grid-assisted wind-hydrogen system. Energy Convers Manag 2018;166:402–8. https://doi.org/10.1016/j.enconman.2018.04.047.

[9]   Abdalla AM, Hossain S, Azad AT, Petra PMI, Begum F, Eriksson SG, et al. Nanomaterials for solid oxide fuel cells: A review. Renew Sustain Energy Rev 2018;82:353–68. https://doi.org/10.1016/J.RSER.2017.09.046.

[10]   Abedin MJ, Masjuki HH, Kalam MA, Sanjid A, Rahman SMA, Masum BM. Energy balance of internal combustion engines using alternative fuels. Renew Sustain Energy Rev 2013;26:20–33.

[11]   Accardo G, Frattini D, Yoon SP, Ham HC, Nam SW. Performance and properties of anodes reinforced with metal oxide nanoparticles for molten carbonate fuel cells. J Power Sources 2017;370:52–60. https://doi.org/10.1016/J.JPOWSOUR.2017.10.015.

[12]   Pianko-Oprych P, Hosseini SM. Dynamic Analysis of Load Operations of Two-Stage SOFC Stacks Power Generation System. Energies 2017, Vol 10, Page 2103 2017;10:2103. https://doi.org/10.3390/EN10122103.

[13]   Azizi MA, Brouwer J. Progress in solid oxide fuel cell-gas turbine hybrid power systems: System design and analysis, transient operation, controls and optimization. Appl Energy 2018;215:237–89. https://doi.org/10.1016/J.APENERGY.2018.01.098.

[14]   Badur J, Lemański M, Kowalczyk T, Ziółkowski P, Kornet S. Verification of zero-dimensional model of SOFC with internal fuel reforming for complex hybrid energy cycles. Chem Process Eng 2018;Vol. 39:113--128. https://doi.org/10.24425/119103.

[15]   Barelli L, Bidini G, Cinti G, Ottaviano A. Study of SOFC-SOE transition on a RSOFC stack. Int J Hydrogen Energy 2017;42:26037–47. https://doi.org/10.1016/J.IJHYDENE.2017.08.159.

[16]   Campanella S, Bracconi M, Donazzi A. A fast regression model for the interpretation of electrochemical impedance spectra of Intermediate Temperature Solid Oxide Fuel Cells. J Electroanal Chem 2018;823:697–712. https://doi.org/10.1016/j.jelechem.2018.06.037.

[17]   Chakravorty J, Sharma G, Bhatia V. Analysis of a DVR with Molten Carbonate Fuel Cell and Fuzzy Logic Control. Technol Appl Sci Res 2018;8:2673–9.

[18]   Danilov NA, Tarutin AP, Lyagaeva JG, Pikalova EY, Murashkina AA, Medvedev DA, et al. Affinity of YBaCo4O7+δ-based layered cobaltites with protonic conductors of cerate-zirconate family. Ceram Int 2017;43:15418–23. https://doi.org/10.1016/J.CERAMINT.2017.08.083.

[19]   de Escalona JMM, Escalona M De, José M, de Escalona JMM. The potential of the supercritical carbon dioxide cycle in high temperature fuel cell hybrid systems. Supercrit CO2 Power Cycle Symp 2011.

[20]   Lorenzo G De, Fragiacomo P. Electrical and thermal analysis of an intermediate temperature {IIR}-{SOFC} system fed by biogas. Energy Sci Eng 2018;6:60–72. https://doi.org/10.1002/ese3.187.

[21]   Dzierzgowski K, Wachowski S, Gojtowska W, Lewandowska I, Jasiński P, Gazda M, et al. Praseodymium

substituted lanthanum orthoniobate: Electrical and structural properties. Ceram Int 2018;44:8210–5. https://doi.org/10.1016/J.CERAMINT.2018.01.270.

[22] El-Hay EA, El-Hameed MA, El-Fergany AA. Steady-state and dynamic models of solid oxide fuel cells based on Satin Bowerbird Optimizer. Int J Hydrogen Energy 2018;43:14751–61. https://doi.org/10.1016/j.ijhydene.2018.06.032.

[23] Ferrel-Álvarez AC, Domínguez-Crespo MA, Cong H, Torres-Huerta AM, Brachetti-Sibaja SB, De La Cruz W. Synthesis and surface characterization of the La0.7-xPrxCa0.3MnO3 (LPCM) perovskite by a non-conventional microwave irradiation method. J Alloys Compd 2018;735:1750–8. https://doi.org/10.1016/J.JALLCOM.2017.11.306.

[24] Genc O, Toros S, Timurkutluk B. Geometric optimization of an ejector for a 4 kW SOFC system with anode off-gas recycle. Int J Hydrogen Energy 2018;43:9413–22. https://doi.org/10.1016/J.IJHYDENE.2018.03.213.

[25] Jienkulsawad P, Saebea D, Patcharavorachot Y, Kheawhom S, Arpornwichanop A. Analysis of a solid oxide fuel cell and a molten carbonate fuel cell integrated system with different configurations. Int J Hydrogen Energy 2018;43:932–42. https://doi.org/10.1016/J.IJHYDENE.2017.10.168.

[26] Kupecki J, Motyliński K, Skrzypkiewicz M, Wierzbicki M, Naumovich Y. Preliminary electrochemical characterization of anode supported solid oxide cell (AS-SOC) produced in the Institute of Power Engineering operated in electrolysis mode (SOEC). Arch Thermodyn 2017;Vol. 38:53–-63. https://doi.org/10.1515/AOTER-2017-0024.

[27] Kupecki J, Skrzypkiewicz M, Motylinski K. Variant analysis of the efficiency of industrial scale power station based on DC-SOFCs and DC-MCFCs. Energy 2018;156:292–8. https://doi.org/10.1016/j.energy.2018.05.078.

[28] Ławryńczuk M. Towards Reduced-Order Models of Solid Oxide Fuel Cell. Complexity 2018;2018. https://doi.org/10.1155/2018/6021249.

[29] Lee D, Cheon Y, Ryu JH, Lee IB. An MCFC operation optimization strategy based on PID auto-tuning control. Int J Hydrogen Energy 2017;42:25518–30. https://doi.org/10.1016/J.IJHYDENE.2017.08.184.

[30] Li Y, Zhang W, Zheng Y, Chen J, Yu B, Chen Y, et al. Controlling cation segregation in perovskite-based electrodes for high electro-catalytic activity and durability. Chem Soc Rev 2017;46:6345–78. https://doi.org/10.1039/C7CS00120G.

[31] Lyagaeva J, Danilov N, Tarutin A, Vdovin G, Medvedev D, Demin A, et al. Designing a protonic ceramic fuel cell with novel electrochemically active oxygen electrodes based on doped Nd0.5Ba0.5FeO3-$\updelta$. Dalt Trans 2018;47:8149–57. https://doi.org/10.1039/c8dt01511b.

[32] A. McClung K. Brun, Chordia L. Technical and economic evaluation of supercritical oxy-combustion for power generation. 4th Int Symp - Supercrit CO2 Power Cycles 2014.

[33] Nadar A, Banerjee AM, Pai MR, Pai R V., Meena SS, Tewari R, et al. Catalytic properties of dispersed iron oxides Fe2O3/MO2 (M = Zr, Ce, Ti and Si) for sulfuric acid decomposition reaction: Role of support. Int J Hydrogen Energy 2018;43:37–52. https://doi.org/10.1016/J.IJHYDENE.2017.10.163.

[34] Peksen M. Safe heating-up of a full scale SOFC system using 3D multiphysics modelling optimisation. Int J Hydrogen Energy 2018;43:354–62. https://doi.org/10.1016/J.IJHYDENE.2017.11.026.

[35] Prokop TA, Berent K, Iwai H, Szmyd JS, Brus G. A three-dimensional heterogeneity analysis of electrochemical energy conversion in {SOFC} anodes using electron nanotomography and mathematical modeling. Int J Hydrogen Energy 2018;43:10016–30. https://doi.org/10.1016/j.ijhydene.2018.04.023.

[36] Zheng Y, Luo Y, Shi Y, Cai N. Dynamic Processes of Mode Switching in Reversible Solid Oxide Fuel Cells. J Energy Eng 2017;143:04017057. https://doi.org/10.1061/(ASCE)EY.1943-7897.0000482.

[37] Fukuzumi S, Lee Y, ChemSusChem WN-, 2017 undefined. Fuel production from seawater and fuel cells using seawater. CbsEwhaAcKr n.d.

[38] Senseni AZ, Meshkani F, Fattahi SMS, Rezaei M. A theoretical and experimental study of glycerol steam reforming over Rh/{MgAl} 2 O 4 catalysts. Energy Convers Manag 2017;154:127–37. https://doi.org/10.1016/j.enconman.2017.10.033.

[39] Xing X, and Jin Lin, Song Y, Zhou Y, Mu S, Hu Q, et al. Modeling and operation of the power-to-gas system

for renewables integration: a review. {CSEE} J Power Energy Syst 2018;4:168–78. https://doi.org/10.17775/cseejpes.2018.00260.

[40] Zhuang Q, Geddis P, Runstedtler A, Clements B. An integrated natural gas power cycle using hydrogen and carbon fuel cells. Fuel 2017;209:76–84. https://doi.org/10.1016/J.FUEL.2017.07.080.

[41] Chen Y, Mojica F, Li G, Chuang P-YA. Experimental study and analytical modeling of an alkaline water electrolysis cell. Int J Energy Res 2017;41:2365–73. https://doi.org/10.1002/ER.3806.

[42] Zhang C, Liu Q, Wu Q, Zheng Y, Zhou J, Tu Z, et al. Modelling of solid oxide electrolyser cell using extreme learning machine. Electrochim Acta 2017;251:137–44. https://doi.org/10.1016/J.ELECTACTA.2017.08.113.

[43] Krawczyk P, Szabłowski Ł, Karellas S, Kakaras E, Badyda K. Comparative thermodynamic analysis of compressed air and liquid air energy storage systems. Energy 2018;142:46–54. https://doi.org/10.1016/J.ENERGY.2017.07.078.

[44] Szablowski L, Krawczyk P, Badyda K, Karellas S, Kakaras E, Bujalski W. Energy and exergy analysis of adiabatic compressed air energy storage system. Energy 2017;138:12–8. https://doi.org/10.1016/J.ENERGY.2017.07.055.

[45] Venkataramani G, Ramalingam V, Viswanathan K. Harnessing Free Energy From Nature For Efficient Operation of Compressed Air Energy Storage System and Unlocking the Potential of Renewable Power Generation. Sci Rep 2018;8. https://doi.org/10.1038/s41598-018-28025-5.

[46] Leśko M, Bujalski W. Modeling of district heating networks for the purpose of operational optimization with thermal energy storage. Arch Thermodyn 2017;Vol. 38:139–-163. https://doi.org/10.1515/AOTER-2017-0029.

[47] Olivier P, Bourasseau C, Bouamama PB. Low-temperature electrolysis system modelling: A review. Renew Sustain Energy Rev 2017;78:280–300. https://doi.org/10.1016/J.RSER.2017.03.099.

[48] Samanta S, Ghosh S. Techno-economic assessment of a repowering scheme for a coal fired power plant through upstream integration of SOFC and downstream integration of MCFC. Int J Greenh Gas Control 2017;64:234–45. https://doi.org/10.1016/J.IJGGC.2017.07.020.

[49] Feher EG. The supercritical thermodynamic power cycle. Energy Convers 1968;8:85–90. https://doi.org/http://dx.doi.org/10.1016/0013-7480(68)90105-8.

[50] Dostal V, Driscoll MJ, Hejzar P. A Supercritical Carbon Dioxide Cycle for Next Generation Nuclear Reactors. Adv Nucl Power Technol Progr 2004.

[51] Driscoll MJ. Supercritical CO2 Plant Cost Assessment 2004.

[52] Chen Y, Lundqvist P, Johansson A, Platell P. A comparative study of the carbon dioxide transcritical power cycle compared with an organic rankine cycle with {R123} as working fluid in waste heat recovery. Appl Therm Eng 2006;26:2142–7. https://doi.org/http://dx.doi.org/10.1016/j.applthermaleng.2006.04.009.

[53] Vidhi R, Goswami DY, Chen H, Stefanakos E, Kuravi S, Sabau AS. Study of supercritical carbon dioxide power cycle for low grade heat conversion. Proc SCO2 Power Cycle Symp 2011:0–7.

[54] Akbari AD, Mahmoudi SMS. Thermoeconomic analysis and optimization of the combined supercritical {CO2} (carbon dioxide) recompression Brayton/organic Rankine cycle. Energy 2014;78:501–12. https://doi.org/http://dx.doi.org/10.1016/j.energy.2014.10.037.

[55] Wang J, Sun Z, Dai Y, Ma S. Parametric optimization design for supercritical {CO2} power cycle using genetic algorithm and artificial neural network. Appl Energy 2010;87:1317–24. https://doi.org/http://dx.doi.org/10.1016/j.apenergy.2009.07.017.

[56] Bryant JC, Saari H, Zanganeh K. An Analysis and Comparison of the Simple and Recompression Supercritical CO2 Cycles. Supercrit CO2 Power Cycle Symp 2011:1–8.

[57] Kim YM, Kim CG, Favrat D. Transcritical or supercritical {CO2} cycles using both low- and high-temperature heat sources. Energy 2012;43:402–15. https://doi.org/http://dx.doi.org/10.1016/j.energy.2012.03.076.

[58] Moroz L, Burlaka M, Rudenko O. Study of a Supercritical CO2 Power Cycle Application in a Cogeneration Power Plant n.d.

[59] Moisseytsev A, Sienicki JJ. Investigation of alternative layouts for the supercritical carbon dioxide

Brayton cycle for a sodium-cooled fast reactor. Nucl Eng Des 2009;239:1362–71. https://doi.org/http://dx.doi.org/10.1016/j.nucengdes.2009.03.017.

[60] Pérez-Pichel GD, Linares JI, Herranz LE, Moratilla BY. Thermal analysis of supercritical {CO2} power cycles: Assessment of their suitability to the forthcoming sodium fast reactors. Nucl Eng Des 2012;250:23–34. https://doi.org/http://dx.doi.org/10.1016/j.nucengdes.2012.05.011.

[61] Harvego EA, McKellar MG. Optimization and Comparison of Direct and Indirect Supercritical Carbon Dioxide Power Plant Cycles for Nuclear Applications. ASME 2011 Int Mech Eng Congr Expo IMECE 2011 2012;4:75–81. https://doi.org/10.1115/IMECE2011-63073.

[62] Halimi B, Suh KY. Computational analysis of supercritical {CO2} Brayton cycle power conversion system for fusion reactor. Energy Convers Manag 2012;63:38–43. https://doi.org/http://dx.doi.org/10.1016/j.enconman.2012.01.028.

[63] Yoon HJ, Ahn Y, Lee JI, Addad Y. Potential advantages of coupling supercritical {CO2} Brayton cycle to water cooled small and medium size reactor. Nucl Eng Des 2012;245:223–32. https://doi.org/http://dx.doi.org/10.1016/j.nucengdes.2012.01.014.

[64] Yamaguchi H, Zhang XR, Fujima K, Enomoto M, Sawada N. Solar energy powered Rankine cycle using supercritical {CO2}. Appl Therm Eng 2006;26:2345–54. https://doi.org/http://dx.doi.org/10.1016/j.applthermaleng.2006.02.029.

[65] Zhang XR, Yamaguchi H, Uneno D, Fujima K, Enomoto M, Sawada N. Analysis of a novel solar energy-powered Rankine cycle for combined power and heat generation using supercritical carbon dioxide. Renew Energy 2006;31:1839–54. https://doi.org/http://dx.doi.org/10.1016/j.renene.2005.09.024.

[66] Zhang XR, Yamaguchi H, Uneno D. Experimental study on the performance of solar Rankine system using supercritical CO2. Renew Energy 2007;32:2617–28. https://doi.org/10.1016/J.RENENE.2007.01.003.

[67] Liu J, Chen H, Xu Y, Wang L, Tan C. A solar energy storage and power generation system based on supercritical carbon dioxide. Renew Energy 2014;64:43–51. https://doi.org/http://dx.doi.org/10.1016/j.renene.2013.10.045.

[68] Iverson BD, Conboy TM, Pasch JJ, Kruizenga AM. Supercritical CO2 Brayton cycles for solar-thermal energy. Appl Energy 2013;111:957–70.

[69] Padilla RV, Too YCS, Benito R, Stein W. Exergetic analysis of supercritical {CO2} Brayton cycles integrated with solar central receivers. Appl Energy 2015;148:348–65. https://doi.org/http://dx.doi.org/10.1016/j.apenergy.2015.03.090.

[70] Cheang VT, Hedderwick RA, McGregor C. Benchmarking supercritical carbon dioxide cycles against steam Rankine cycles for Concentrated Solar Power. Sol Energy 2015;113:199–211. https://doi.org/http://dx.doi.org/10.1016/j.solener.2014.12.016.

[71] Czelej K, Cwieka K, Colmenares JC, Kurzydlowski KJ. Atomistic insight into the electrode reaction mechanism of the cathode in molten carbonate fuel cells. J Mater Chem A 2017;5:13763–8. https://doi.org/10.1039/C7TA02011B.

[72] Sánchez D, Chacartegui R, Jiménez-Espadafor F, Sánchez T. A New Concept for High Temperature Fuel Cell Hybrid Systems Using Supercritical Carbon Dioxide. J Fuel Cell Sci Technol 2009;6:1–11.

[73] de Escalona JMM. The potential of the supercritical carbon dioxide cycle in high temperature fuel cell hybrid systems. Supercrit CO2 Power Cycle Symp 2011.

[74] Bae SJ, Ahn Y, Lee J, Lee JI. Various supercritical carbon dioxide cycle layouts study for molten carbonate fuel cell application. J Power Sources 2014;270:608–18. https://doi.org/10.1016/j.jpowsour.2014.07.121.

[75] Grzebielec A, Rusowicz A, Szelągowski A. Air purification in industrial plants producing automotive rubber components in terms of energy efficiency. Open Eng 2017;7:106–14. https://doi.org/10.1515/ENG-2017-0015.

[76] Le Moullec Y. Conceptual study of a high efficiency coal-fired power plant with CO2 capture using a supercritical CO2 Brayton cycle. Energy 2013;49:32–46. https://doi.org/10.1016/J.ENERGY.2012.10.022.

[77] Audasso E, Nam S, Arato E, Bosio B. Preliminary model and validation of molten carbonate fuel cell kinetics under sulphur poisoning. J Power Sources 2017;352:216–25.

https://doi.org/10.1016/J.JPOWSOUR.2017.03.091.

[78] Le Moullec Y. Conception of a Pulverized Coal Fired Power Plant with Carbon Capture around a Supercritical Carbon Dioxide Brayton Cycle. Energy Procedia 2013;37:1180–6. https://doi.org/10.1016/J.EGYPRO.2013.05.215.

[79] Chen Y, Lundqvist P, Johansson A, Platell P. A comparative study of the carbon dioxide transcritical power cycle compared with an organic Rankine cycle with R123 as working fluid in waste heat recovery. Appl Therm Eng 2006;26:2142–7.

[80] Chen Y, Lundqvist P, Platell P. Theoretical research of carbon dioxide power cycle application in automobile industry to reduce vehicle's fuel consumption. Appl Therm Eng 2005;25:2041–53. https://doi.org/http://dx.doi.org/10.1016/j.applthermaleng.2005.02.001.

[81] Vaclav Dostal by, Coderre JA. A Supercritical Carbon Dioxide Cycle for Next Generation Nuclear Reactors Certified by A � A Chairman, Department Committee on Graduate Students. Dipl Ing, Mech Eng 2000.

[82] Chapman D, Arias D. An Assessment of the Supercritical Carbon Dioxide Cycle for Use in a Solar Parabolic Trough Power Plant. Proc o SCCO2 Power Cycle Symp 2009.

[83] Vidhi R, Goswami YD, Chen H, Stefanakos E, Kuravi S, Sabau AS. Study of Supercritical Carbon Dioxide Power Cycle for Low Grade Heat Conversion 2011.

[84] Angelino G. Carbon Dioxide Condensation Cycles for Power Production. ASME Pap No 68-GT-23 1968.

[85] Oda E, Abdelsalam A, … MA-W-ASE, 2017 undefined. Distributed generations planning using flower pollination algorithm for enhancing distribution system voltage stability. Elsevier n.d.

[86] Sultana S, Roy PK. Krill herd algorithm for optimal location of distributed generator in radial distribution system. Appl Soft Comput 2016;40:391–404. https://doi.org/10.1016/J.ASOC.2015.11.036.

[87] Kansal S, Kumar V, Tyagi B. Hybrid approach for optimal placement of multiple DGs of multiple types in distribution networks. Int J Electr Power Energy Syst 2016;75:226–35. https://doi.org/10.1016/J.IJEPES.2015.09.002.

[88] El-Fergany A. Multi-objective Allocation of Multi-type Distributed Generators along Distribution Networks Using Backtracking Search Algorithm and Fuzzy Expert Rules. Http://DxDoiOrg/101080/1532500820151102989 2015;44:252–67. https://doi.org/10.1080/15325008.2015.1102989.

[89] Rajendran A, Narayanan K. Optimal multiple installation of DG and capacitor for energy loss reduction and loadability enhancement in the radial distribution network using the hybrid WIPSO–GSA algorithm. Https://DoiOrg/101080/0143075020181451371 2018;41:129–41. https://doi.org/10.1080/01430750.2018.1451371.

[90] Rama Prabha D, Jayabarathi T. Optimal placement and sizing of multiple distributed generating units in distribution networks by invasive weed optimization algorithm. Ain Shams Eng J 2016;7:683–94. https://doi.org/10.1016/J.ASEJ.2015.05.014.

[91] Ganguly S, Samajpati D. Distributed generation allocation with on-load tap changer on radial distribution networks using adaptive genetic algorithm. Appl Soft Comput 2017;59:45–67. https://doi.org/10.1016/J.ASOC.2017.05.041.

[92] Tolba MA, Zaki Diab AA, Vanin AS, Tulsky VN, Abdelaziz AY. Integration of Renewable Distributed Generation in Distribution Networks Including a Practical Case Study Based on a Hybrid PSOGSA Optimization Algorithm. Https://DoiOrg/101080/1532500820181532470 2019;46:2103–16. https://doi.org/10.1080/15325008.2018.1532470.